Enhancing carrier injection in the active region of a 280nm emission wavelength LED using graded hole and electron blocking layers.

Bilal Janjua[a], Tien K. Ng[a], Ahmed Y. Alyamani[b], Munir M. El-Desouki[b] and Boon S. Ooi*[a]
[a]Photonics Laboratory, King Abdullah University of Science & Technology (KAUST), Thuwal 23955-6900, Kingdom of Saudi Arabia (KSA)
[b]King Abdulaziz City for Science and Technology (KACST), Riyadh, 11442-6086, Kingdom of Saudi Arabia (KSA)

ABSTRACT

A theoretical investigation of AlGaN UV-LED with band engineering of hole and electron blocking layers (HBL and EBL, respectively) was conducted with an aim to improve injection efficiency and reduce efficiency droop in the UV LEDs. The analysis is based on energy band diagrams, carrier distribution and recombination rates (Shockley-Reed-Hall, Auger, and radiative recombination rates) in the quantum well, under equilibrium and forward bias conditions. Electron blocking layer is based on $Al_aGa_{1-a}N$ / $Al_{b \rightarrow c}Ga_{1-b \rightarrow 1-c}N$ / $Al_dGa_{1-d}N$, where a > d > b > c. A graded layer sandwiched between large bandgap AlGaN materials was found to be effective in simultaneously blocking electrons and providing polarization field enhanced carrier injection. The graded interlayer reduces polarization induced band bending and mitigates the related drawback of impediment of holes injection. Similarly on the n-side, the $Al_{x \rightarrow y}Ga_{1-x \rightarrow 1-y}N$ / $Al_zGa_{1-z}N$ (x < z < y) barrier acts as a hole blocking layer. The reduced carrier leakage and enhanced carrier density in the active region results in significant improvement in radiative recombination rate compared to a structure with the conventional rectangular EBL layers. The improvement in device performance comes from meticulously designing the hole and electron blocking layers to increase carrier injection efficiency. The quantum well based UV-LED was designed to emit at 280nm, which is an effective wavelength for water disinfection application.

Keywords: Light emitting diodes (LEDs), nitride, quantum well, graded layer, carrier leakage, ultraviolet, water disinfection and numerical simulation.

1. INTRODUCTION

AlGaN based UV LEDs have attracted great attention for applications in environmental cleansing, medicine, lighting, *etc*. [1]. Due to high polarization fields and large defect density, the illumination power and internal efficiency of nitride based devices is low [2, 3, 4, 5, 6, 7]. Due to low doping efficiencies, in such UV LEDs, enhancing carrier injection in the active region remains a great challenge [8, 9]. To improve internal quantum efficiency, grading has been used in InGaN/AlInGaN quantum wells (QW) based LEDs [10, 11, 12] with reported 5-6 times enhancement in radiative recombination. Currently, grading schemes have improved carrier injection [10, 13, 14], and doping [15] in UV-LEDs emitting around 280nm. To date, UV LEDs were championed by SETI Corporation with record external efficiency of more than 11% at 278nm emission wavelength [16]. Design rules are not well established due to complicated relation between polarization field, lattice strain, defects and bandgap engineering. This requires a careful simulation of the layer structure before realization of actual device growth. Design based on the actual allowable growth related boundary conditions is hence vital to the usefulness of a simulation. This paper explores graded barrier layer design with eventual view of realizing the design using plasma source molecular beam epitaxy (PAMBE).

Band bending, in presence of strong polarization field's, results in reduced oscillator strength of carrier transitions, a dimensionless quantity, expressing the strength of direct transition, and the Quantum Confined Stark Effect (QCSE). Band bending causes large carrier leakage losses, which can be mitigated via use of carrier blocking layers on the p-side of the device [17]. Conventional blocking layer based on rectangular band gap design have a drawback of obstructing

*boon.ooi@kaust.edu.sa; http://photonics.kaust.edu.sa

Light-Emitting Diodes: Materials, Devices, and Applications for Solid State Lighting XVIII, edited by Klaus P. Streubel, Heonsu Jeon, Li-Wei Tu, Martin Strassburg, Proc. of SPIE Vol. 9003, 90030S
 · doi: 10.1117/12.2039347

flow of both types of carrier, which are electrons and holes [18]. Designs based on low band gap intermediate layers, in and around the electron blocking layer (EBL), have proven to be useful in increasing carrier injection [13,19,20]. Small valence band offset in AlGaN based single quantum well structures (SQW) further reduces carrier confinement, causing spillover of carrier out of the active region [21]. This requires careful designing of barrier layers and incorporating novel schemes based on compositional grading. Such designs are yet to be fully developed in conjunction with AlGaN SQW grown device using PAMBE, which has a controllable growth rate of < 1 nm per minute, favoring the implementation of the compositional graded layers.

In this paper, the design of electron-blocking layer (EBL) and hole-blocking layer (HBL), based on band engineering, has been studied numerically. The analysis considered energy band structure, carrier densities, recombination rates and optical transition oscillatory strength. Polarization induced band bending due to interface fixed charges was incorporated. The band diagram of the structure was obtained by solving Poisson's, Schrödinger, current continuity, carrier transport and photon rate equation, self-consistently. Ohmic, *n* and *p* contacts were used for simplicity. Doping dependent nobilities were obtained using Arora model, built in the numerical software.

The graded barriers were optimized to maximize carrier densities in the active region. Comparing conventional rectangular barriers design and the proposed design, we found a significant enhancement in radiative recombination rate due to improved carrier injection.

The proposed UV-LED is designed to emit at 280nm, which is an attractive wavelength for water disinfection applications. Proposed designed was modeled using the NEXTNANO software [22].

2. Device Structure

III-Nitride based material systems have strong spontaneous and piezoelectric polarization fields, which result in large band bending. In order to overcome the energy barrier introduced by the high polarization fields, designs based on graded barriers can be an effective way in blocking one type of carrier while introducing minimum resistance to the other carrier type.

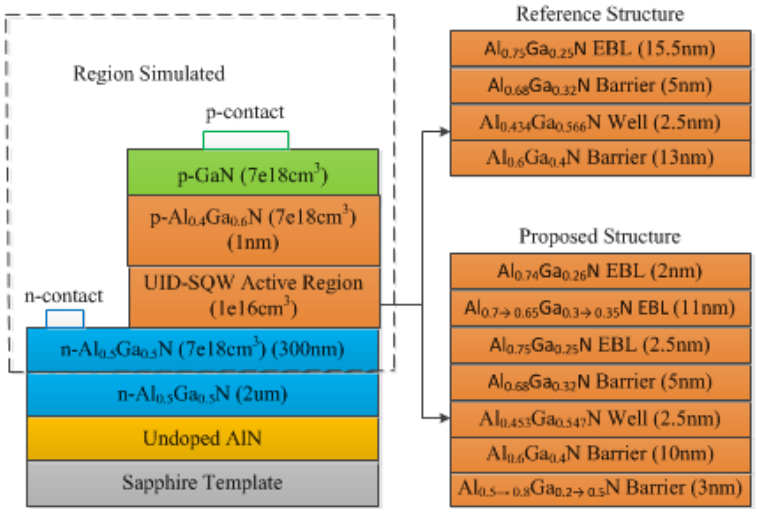

Fig. 1: Schematics of reference design, and proposed design with graded barrier layers.

The proposed design based on $Al_{x \rightarrow y}Ga_{1-x \rightarrow 1-y}N$ / $Al_zGa_{1-z}N$ (x < z < y) HBL on n-side and $Al_aGa_{1-a}N$ / $Al_{b \rightarrow c}Ga_{1-b \rightarrow 1-c}N$ / $Al_dGa_{1-d}N$, where a > d > b > c, EBL on p-side, is shown in Fig. 1. The LED modeled in this study consists of a 200nm

$Al_{0.5}Ga_{0.5}N$ buffer layer, n doped, with carrier concentration 7e18cm^3. The active region consists of 3nm graded hole blocking layer (HBL) $Al_{0.5\rightarrow0.8}Ga_{0.5\rightarrow0.2}N$ followed by a 10nm bottom $Al_{0.6}Ga_{0.4}N$ barrier. Next to barrier layer, is a 2.5nm $Al_{0.453}Ga_{0.547}N$ QW designed to emit at 280nm, terminated with a 5nm $Al_{0.68}Ga_{0.32}N$ top barrier. The asymmetric barrier design around the well was chosen to take into account differences in mobility of holes and electrons. The electron blocking layer (EBL) consists of a 10nm graded $Al_{0.7\rightarrow0.65}Ga_{0.3\rightarrow0.35}N$ layer sandwiched between two AlGaN layers with aluminum (Al) mole fraction of 75% and 74% and thickness of 2.5nm and 2nm. The graded EBL design was adopted to minimize energy barrier, which hole have to overcome in reaching the QW. Active region is assigned an unintentional background electron carrier concentration of 1e16cm^{-3} to prevent doping induced non-radiative recombination and impurity scattering. A low bandgap $Al_{0.4}Ga_{0.6}N$ layer was inserted between EBL and p-GaN layer as it is shown to enhance hole injection into the active region [13]. The p-GaN was assigned a hole concentration of 7e18cm^{-3}.

3. Numerical Simulation Setup

The material parameters of AlGaN ternary alloys are expressed as:

$$X\left(Al_xGa_{1-x}N\right)=x.X\left(AlN\right)+\left(1-x\right).X\left(GaN\right)-b.x.(1-x)$$

where, b is the bowing parameter and $X(AlN)$ and $X(GaN)$ are the material parameters of binaries aluminum nitride (AlN) and gallium nitride(GaN) with values mentioned in table 1 [5].

Table. 1: Material properties of the binary used in the simulation with bowing parameters.

Material	**E_g at 0K**	**a(nm)**	**c(nm)**	**Spontaneous Polarization (Cm^{-2})**
AlN	6.1	0.3112	0.4982	-0.0898
GaN	3.51	0.31892	0.5185	-0.0339
Bowing parameter (b)	0.8	-0.007	0.039	-0.021

Electron and holes, band masses, elastic, piezoelectric, deformation potentials and 6x6k.p parameters are taken from ref. 2 to 5. Materials properties, with no bowing parameters, are interpolated linearly for ternary. For electrons, effective mass approximation was used to calculate bands, to reduce numerical computational complexity. Valence bands are calculated using 6x6k.p. Valence band offset was set to 0.85eV for GaN layer lattice matched to AlN, taking into account strain and polarization induced band bending effect. Operating temperature of the device is taken to be 300K. All layers are assumed to be pseudomorphic on $Al_{0.5}Ga_{0.5}N$ buffer layer.

The Arora approximation introduced to depict the mobility as a function of carrier density, also takes into account scattering by charged impurities ions and is modeled as:

$$u\left(T,N_i\right)=u_{min}{}^{n,p}\left(\frac{T}{T_o}\right)^{\alpha_m{}^{n,p}}+\frac{u_d{}^{n,p}\left(\frac{T}{T_o}\right)^{\alpha_d{}^{n,p}}}{1+\left(\frac{N_D+N_A}{N_0{}^{n,p}\left(\frac{T}{T_o}\right)^{\alpha_N{}^{n,p}}}\right)^{A_a{}^{n,p}\left(\frac{T}{T_o}\right)^{\alpha_a{}^{n,p}}}}$$

where $u_{min}, u_d, \alpha_m, \alpha_d, \alpha_N, \alpha_a, N_0$ are Arora model fitting parameters [23, 24]. $N_A + N_D$ is the total concentration of ionized impurities. Fitting parameters used; take into account dislocation density of 1e18cm^{-2} for electrons and 0cm^{-2} for holes. In AlN, fitting parameters are assumed to be the same as GaN, due to non-availability of data.

4. Results and Discussion

In order to understand the carrier dynamics inside the active region, one has to study the band diagram of the device. Figure 2 shows the conduction and valence bands with their corresponding quasi Fermi levels.

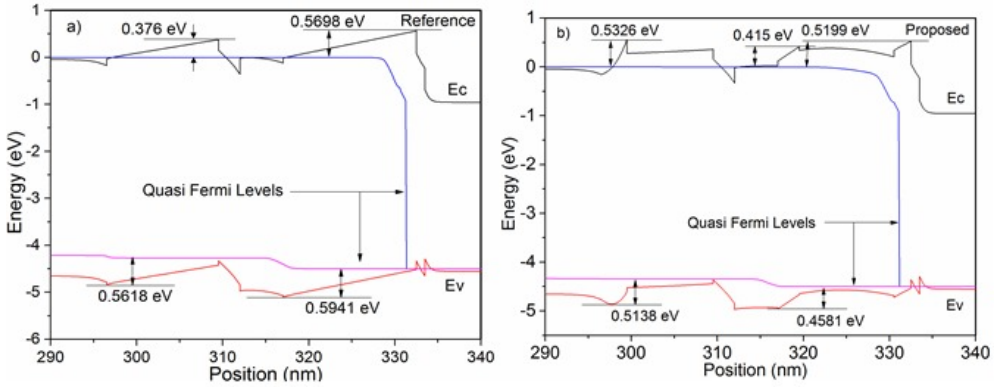

Fig. 2: Energy band diagram of reference and proposed structure under forward bias of 4.5eV.

As shown in Fig. 2, the effective barrier height introduced by EBL for electrons, in proposed structure, is slightly reduced from 0.5698eV to 0.415eV. This will lead to unwanted escape of electrons from the active region. For reference structure, as shown in Figure 2a, where the barrier height gradually increases across the EBL; the proposed structure has a more abrupt energy barrier profile. This enhances electron reflection closer to the QW and reduced non radiative recombination in the EBL. For holes, in the reference structure, the EBL introduces a barrier height of 0.5941eV which can lead to poor injection efficiency. In our proposed structure, band bending due to the induced volume charge by Al compositional grading, considerably reduces the energy barrier by 0.136eV, thus enhancing hole injection efficiency. For HBL, grading does not lead to significant change in the energy barrier height. This is caused by negligible band bending in the bottom barrier. Electron density, in proposed structure, is slightly reduced in the QW and will be discussed latter in the paper. Graded HBL layer not only provides abrupt energy barrier to holes; it can also act as strain and dislocation relief layer [25].

Electric field profile across the active region, under forward bias, gives a clearer picture of polarization induced fixed charges.

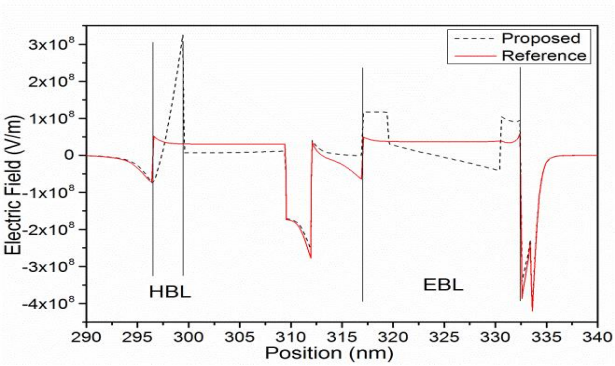

Fig. 3: Electric Field profile across EBL for proposed and reference structure under forward bias of 4.5V.

As seen in Fig 3, our proposed structure, grading in EBL creates an electric field with negative gradient and magnitude. This causes negative bending in valence band inside the EBL resulting in reduced barrier height for holes to overcome. For HBL, switch in electric field sign due to polarization induced volume charges, causes a hump in energy profile of valence band. Reduced electric field in top barrier, of proposed structure, results in absence of two dimensional electron gas (2DEG) formation at the top barrier EBL interface. Inside the QW, electric field profile is negligibly altered when using the graded scheme in the carrier blocking layers.

Wavefunction profile gives an idea about the extent of carrier confinement in the active region. Stronger confinement leads to more efficient radiative recombination process. Figure 4 shows the carrier wave functions profile of the fundamental transition state and their corresponding energy band edges.

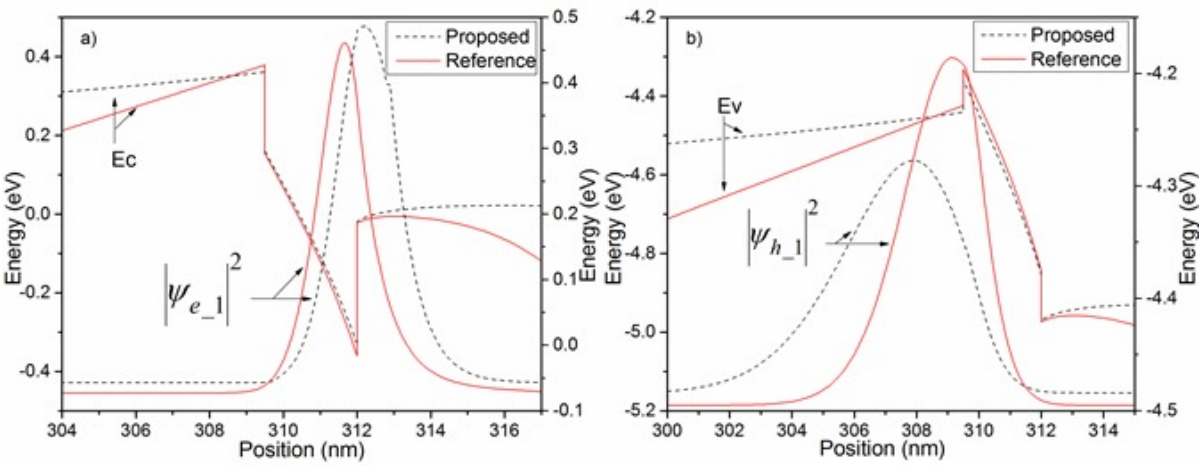

Fig. 4: Wavefunction with their corresponding band edges for a) electrons and b) holes. Quantum well (309.5nm to 312nm).

Strong polarization and small valence band offsets in AlGaN alloys causes considerable separation of carrier in the quantum well. Weakly localized wavefunctions lead to higher non-radiative recombination in the barrier layers.

According to Fermi's golden rule, the transition matrix element is proportional to the square of the electron-hole wave function overlap or spatial overlap matrix element ($|\Psi_{h\_1}|\ \Psi_{e\_1}|^2$). With increase in overlap, the spontaneous radiative recombination is enhanced. Optical matrix element, for proposed structure is 0.038, which is smaller than 0.0932 in reference structure. In the reference structure, due to polarization induced bend bending inside the barrier, layers, wavefunction are more localized inside the QW resulting larger wavefunction overlap values. As can be seen in Fig. 4, the effect of band bending, in barrier layers, is more significant, on the hole wavefunction. Slight shift of eigen values to higher energies, leads to less localized electron wavefunction in the proposed structure. Thus careful engineering of polarization fields, inside the active region, are required to improve carrier separation. Even though the strength of radiative recombination is reduced in the proposed structure, as will be discussed later, the enhanced carrier injection, due to graded blocking layers, leads to overall better performance in proposed structure.

To evaluate the effectiveness of graded barrier, in increasing device performance, carriers being supplied to the QW have to be taken into account. Figure 5 gives the carrier density profile in the QW of proposed and reference structure.

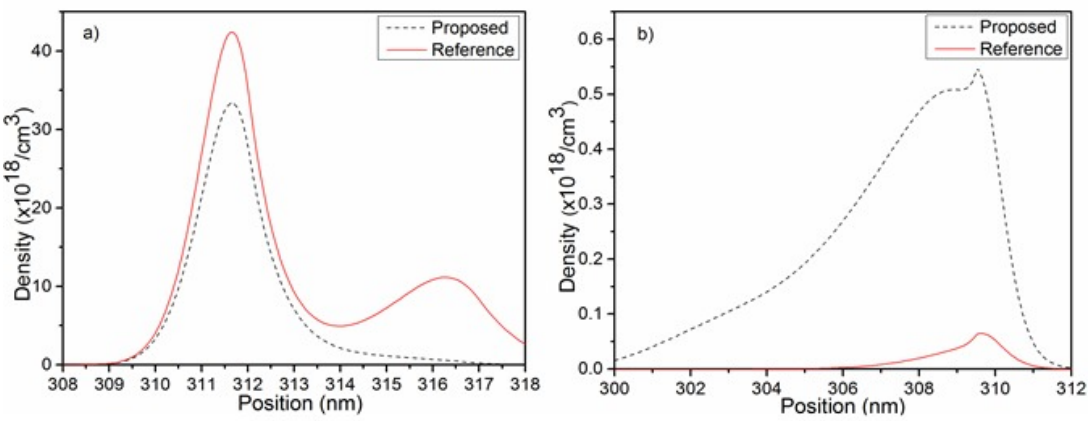

Fig. 5: Carrier densities of (a) electrons and (b) holes, under forward bias of 4.5V, for reference and proposed structure. Quantum well (309.5nm to 312nm).

As can be seen in Fig. 5, compared to holes, the electron density is more localized in the active due to larger conduction band offset and better confinement in presence of large bandgap barrier. Aluminum compositional grading in HBL, slightly reduces the electron concentration in the QW due to introduction of 0.5326eV barrier height as shown in Fig. 2. Reduced electric fields, in the top barrier of proposed structure, results in absence of 2DEG at top barrier and EBL interface. For reference structure, 2DEG formation, as confirmed by increase in electron density in top barrier (312nm to 317nm), can lead to unwanted non-radiative recombination at top barrier EBL interface.

Hole density compared to that of electron, is considerably reduced and can be attributed to smaller valence band offsets and introduction of an energy barrier by EBL. As shown in Fig. 5b, the hole concentration in the proposed structure is noticeably higher than that of reference structure. The drastic increase in hole density observed is due to reduction in energy barrier caused by EBL. Non localization of holes, inside the QW, can also be seen, as the density profile is more spread out into the barrier.

When the carriers are injected into the active region, they can either recombine radiatively or none radiatively. Recombination rates, in the simulation, are modeled as:

$$R_{Tot} = R_{Inj} - (R_{SRH} + R_{Auger} + R_{Direct})$$

where

$$R_{SRH} = \frac{p.n - n_i^2}{\tau_p\left(n + n_i\right) + \tau_n\left(p + n_i\right)},$$

$$R_{Auger} = C_p.(n^2 - n_i^2)p + C_n.(p^2 - n_i^2)n,$$

$$R_{Direct} = C.(n.p - n_i^2),$$

where τ_n, τ_p, C_n and C_p are Shockley Read Hall, Auger and direct radiative recombination rates coefficients. In nitride based devices, Auger recombination term, $C_p.n^2.p$, is dominant, due to poor hole injection efficiency into the active region. The coefficients used to model the recombination rates are tabulated in Table. 3 [12, 26, 27]. At lower carrier injection, recombination is dominated by non-radiative recombination. With increase in forward bias, direct radiative recombination takes over. For very high injection, Auger recombination can be significant. In InGaN based devises auger recombination rate has been considered as a dominant recombination mechanism for droop [28]. Droop refers to reduction in nitride based device performance at high injection levels.

Table: 2. Material coefficients used to model SRH, Auger and direct radiative recombination rates.

Material	Auger Recombination Coefficients (cm^6s^{-1})		SRH Recombination Coefficients (cm^{-3})		Direct Radiative recombination Coefficients cm^3s^{-1}
	C_n	C_p	τ_n	τ_p	
GaN	1.25e-31	5e-32	10e-9	20e-9	0.45e-10
AlN	5e-32	5e-32	5e-9	10e-9	0.18e-10

Auger recombination is a three particle process. With increase in carrier density, Auger recombination rate increases. For large bandgap material, Auger recombination is less significant under lower carrier injection levels, due to relatively smaller recombination rate coefficients. SRH recombination on the other hand is a one particle process which can be significant at lower carrier densities. Unlike Auger, SRH coefficients increases with bandgap as the trap states become closer to the midgap level, thus SRH can be significant at lower injection values.

For UV devices both SRH and Auger can be substantial and cannot be ignored when designing the device.

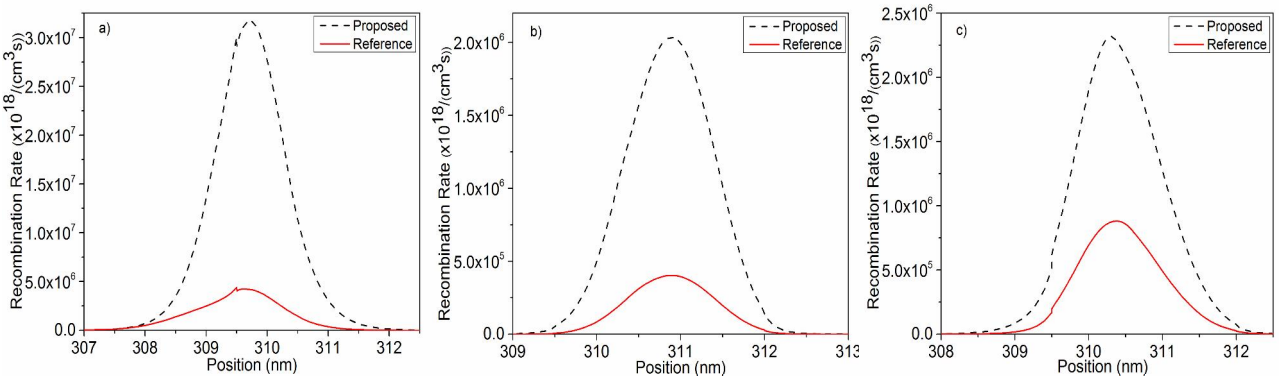

Fig. 6: Recombination rates a) SRH, b) Auger and c) Direct, in the quantum well region (309.5nm-312nm).

Recombination rates for the structures are shown in Fig. 6. With the graded EBL design, due to higher hole injection, direct useful recombination is higher than the reference structure. Direct recombination rate is weighted with the spatial overlap matrix element of the fundamental transition in the QW. SRH being a single particle process takes into account both electrons and holes recombining via trap states. Since holes density is shifted more towards the bottom barrier of QW, SRH peaks on the bottom side of the QW. Auger being a three particle process, is dominated by e-e-h transitions, thus its profile follows that of electron density. SRH and Auger recombination are more severe in our proposed design due to higher carrier density inside the QW.

5. Summary

In this paper, we proposed graded electron and hole blocking layers to enhance device performance of a UV-LED, designed to emit at 280nm. Numerical results show that the hole density, inside the QW, can be significantly increased using graded EBL resulting in stronger useful direct radiative recombination process. Further optimization of polarization fields inside the barrier layers, in reducing carrier separation, can lead to further improvement in device performance.

Acknowledgement

Bilal janjua gratefully acknowledges the financial support from King Abdulaziz City for Science and Technology (KACST), under the Technology Innovation Center (TIC) program.

References

[1] Zhang, J., Chitnis, A., Adivarahan, V., Wu, S., M, Avilli, V., Pachipulusu, R., Shatalov, M., Simin, G., Yang, J. and Khan, M., " Milliwatt power deep ultraviolet light-emitting diodes over sapphire with emission at 278 nm," Applied physics letters, 81 (26), 4910-4912 (2002).
[2] Park, S. and Chuang, S., "Crystal-orientation effects on the piezoelectric field and electronic properties of strained wurtzite semiconductors," Physical Review B, 59 (7), 4725 (1999).
[3] Park, S. and Chuang, S., "Comparison of zinc-blende and wurtzite GaN semiconductors with spontaneous polarization and piezoelectric field effects," Journal of Applied Physics, 87 (1), 353-364 (2000).
[4] Park, S., "Crystal orientation effects on electronic properties of wurtzite GaN/AlGaN quantum wells with spontaneous and piezoelectric polarization," Japanese Journal of Applied Physics, 39, 3478 (2000).
[5] Piprek. J., [Nitride semiconductor devices: principles and simulation], Wiley.com, (2007).
[6] Ambacher, O., "Growth and applications of group III-nitrides," Journal of Physics D: Applied Physics, 31 (20), 2653 (1998).
[7] Sun, H., Woodward, J., Yin, J., Moldawer, A., Pecora, E., Nikiforov, A., Dal Negro, L., Paiella, R., Ludwig, K., Smith, D. and Others., "Development of AlGaN-based graded-index-separate-confinement-heterostructure deep UV emitters by molecular beam epitaxy," Journal of Vacuum Science & Technology B: Microelectronics and Nanometer Structures, 31 (3), 03117-03117 (2013).
[8] Katsuragawa, M., Sota, S., Komori, M., Anbe, C., Takeuchi, T., Sakai, H., Amano, H. and Akasaki, I., "Thermal ionization energy of Si and Mg in AlGaN," Journal of crystal growth, 189, 528-531 (1998).
[9] Stampfl, C., Neugebauer, J. and Van De Walle, C., "Doping of Al xGa1- xN alloys," Materials Science and Engineering: B, 59 (1), 253-257 (1999).
[10] Bour, D. P., Gardner, N. F., Goetz, W. K., Stockman, S. A., Taleuchi, T., Hasnain, G., Kocot, C. P. and Hueschen, M. R., "Light emitting diodes with graded composition active regions," Google Patents (2005).
[11] Zhao, H., Liu, G., Zhang, J., Poplawsky, J., Dierolf, V. and Tansu, N., "Approaches for high internal quantum efficiency green InGaN light-emitting diodes with large overlap quantum wells," Optics express, 19 (104), 991-1007 (2011).
[12] Shur, M. and Gaska, R., "Deep-ultraviolet light-emitting diodes," Electron Devices, IEEE Transactions on, 57 (1), 12-14 (2010).
[13] Liao, Y., Thomidis, C., Kao, C. and Moustakas, T., "AlGaN based deep ultraviolet light emitting diodes with high internal quantum efficiency grown by molecular beam epitaxy," Applied Physics Letters, 98, 081110 (2011).
[14] Johnson, M., Long, J. and Schetzina, J., "New UV Light Emitter Based on AlGaN Heterostructures with Graded Electron and Hole Injectors," Mat. Res. Soc. Symp. Proc, 743, 481-486 (2003).
[15] Zhang, L., Ding, K., Yan, J., Wang, J., Zeng, Y., Wei, T., Li, Y., Sun, B., Duan, R. and Li, J., "Three-dimensional hole gas induced by polarization in (0001)-oriented metal-face III-nitride structure," Applied Physics Letters, 97 (6), 062103-062103 (2010).
[16] Shatalov, M., Sun, W., Lunev, A., Hu, X., Dobrinsky, A., Bilenko, Y., Yang, J., Shur, M., Gaska, R., Moe, C. and Others., "278 nm deep ultraviolet LEDs with 11% external quantum efficiency," Device Research Conference (DRC), 70th Annual, IEEE, 255-256 (2012).
[17] Hirayama, H., Tsukada, Y., Maeda, T. and Kamata, N., "Marked enhancement in the efficiency of deep-ultraviolet AlGaN light-emitting diodes by using a multiquantum-barrier electron blocking layer," Applied Physics Express, 3 (3), 1002 (2010).
[18] Kuo, Y., K., Shih, Y., H., Tsai, M., C. and Chang, J., Y., "Improvement in electron overflow of near-ultraviolet InGaN LEDs by specific design on last barrier," Photonics Technology Letters, IEEE, 23, 1630-1632 (2011).
[19] Tian, W., Feng, Z., Liu, B., Xiong, H., Zhang, J., Dai, J., Cai, S. and Chen, C., "Numerical study of the advantages of ultraviolet light-emitting diodes with a single step quantum well as the electron blocking layer," Optical and Quantum Electronics, 1-7 (2013).
[20] Zhang, J., Tian, W., Wu, F., Yan, W., Xiong, H., Dai, J., Fang, Y., Wu, Z. and Chen, C., "The advantages of AlGaN-based UV-LEDs inserted with a p-AlGaN layer between the EBL and active region," IEEE, 1-1 (2013).
[21] Bernardini, F. and Fiorentini, V., "Macroscopic polarization and band offsets at nitride heterojunctions," Physical

Review B, 57 (16), 9427 (1998).
[22] Birner, S., Hackenbuchner, S., Sabathil, M., Zandler, G., Majewski, J., Andlauer, T., Zibold, T., Morschl, R., Trellakis, A. & Vogl, P," Modeling of Semiconductor Nanostructures with nextnano^3," Acta Physica Polonica Series A, 110, 111 (2006).
[23] Arora, N. D., Hauser, J. R. & Roulston, D. J., "Electron and hole mobilities in silicon as a function of concentration and temperature," Electron Devices, IEEE Transactions on, 29, 292-295 (1982).
[24] Enrico, B., and Bertazzi, F. "Transport parameters for electrons and holes," Wiley-VCH Verlag GmbH & Co. KGaA, Weinheim, Germany, 2007.
[25] TERSOFF, J., " Dislocations and strain relief in compositionally graded layers," *Applied physics letters,* 62**,** 693-695 (1993).
[26] Delaney, K., Rinke, P. and Van De Walle, C., "Auger recombination rates in nitrides from first principles," Applied Physics Letters, 94 (19), 191109-191109 (2009).
[27] Piprek, J., [Semiconductor Optoelectronic Devices], Academic Press, San Diego (2003).
[28] Ivel, Martinelli, L., Peretti, J., Speck, J. and Weisbuch, C., "Direct Measurement of Auger Electrons Emitted from a Semiconductor Light-Emitting Diode under Electrical Injection: Identification of the Dominant Mechanism for Efficiency Droop," Physical review letters, 110 (17), 177406 (2013).